Thickening supercritical CO_2 at high temperatures with rod-like reverse micelles

Masanobu Sagisaka[a,*], *Yuuki Sato*[a], *Sajad Kiani*[b], *Shirin Alexander*[b], *Tretya Ardyani*[c], *Azmi Mohamed*[c,d], *Robert M. Enick*[e], *Sarah E. Rogers*[f], *Christopher Hill*[g,h], *and Julian Eastoe*[h]

[a] Department of Frontier Materials Chemistry, Graduate School of Science and Technology, Hirosaki University, 3 Bunkyo-cho, Hirosaki, Aomori 036-8561, JAPAN

[b] School of Engineering and Applied Sciences, Energy Safety Research Institute (ESRI), Swansea University, Bay Campus, Swansea SA1 8EN, UK

[c] Department of Chemistry, Faculty of Science and Mathematics, Universiti Pendidikan Sultan Idris, 35900 Tanjong Malim, Perak, Malaysia

[d] Nanotechnology Research Centre, Faculty of Science and Mathematics, Universiti Pendidikan Sultan Idris, 35900 Tanjong Malim, Perak, Malaysia

[e] Department of Chemical and Petroleum Engineering, University of Pittsburgh, 940 Benedum Hall, 3700 O'Hara Street, Pittsburgh, Pennsylvania 15261, United States

[f] ISIS-CCLRC, Rutherford Appleton Laboratory, Chilton, Oxon OX11 0QX, U.K.

[g] School of Chemistry, Trinity College Dublin, Dublin 2, Ireland.

[h] School of Chemistry, University of Bristol, Cantock's Close, Bristol BS8 1TS, U.K.

*Corresponding author

19 E-mail addresses: sagisaka@hirosaki-u.ac.jp

Abstract

Earlier studies demonstrated the ability of some fluorinated surfactants to form rod-like reverse micelles with thickening ability in water/supercritical CO_2 ($scCO_2$) mixtures at temperatures below 45 ºC [*Langmuir* 26 (2010) 83-88. *Soft Matter* 8 (2012) 7044–7055. *Colloids and Surfaces B,* 168 (2018), 201-210.]. Such a viscosity enhancement of $scCO_2$ is known to increase sweep efficiency for oil recovery with CO_2 flooding. However, temperatures of up to ~100 ºC in conventional reservoirs are much higher than those studied, and tend to weaken inter- and intra-molecular interactions between surfactant molecules, discouraging rod-like reverse micelle formation. With the aim of designing surfactants which form rod-like reverse micelles and thicken CO_2 at high temperatures, this study examined phase behavior, nanostructures of reverse micelles and thickening ability of double ω-hydroperfluorocarbon-tail anionic surfactants in W/$scCO_2$ mixtures at temperatures of 35 - 75 ºC and 80 - 400 bar with different water-to-surfactant molar ratios (W_0). The measured CO_2 viscosity increased by 1.9-2.2 × for double-chain surfactants M(di-HCF6)$_x$ (counterion M^{x+} = Ni^{2+} and Co^{2+}) at 40 mM, over the experimental temperature range. On the other hand, the shorter chain $H(CF_2)_4CH_2$ twin-tail surfactants M(di-HCF4)$_x$ and Na(di-HCF6) gave only 1.1-1.5 × enhancements. The maximum thickening ability of M(di-HCF6)$_2$ was at W_0 = 10 in the W_0 range of 5-20 75 ºC and 350 bar. High pressure and temperature small-angle neutron scattering (SANS) was used determine the micellar structure in these systems, and rod micelles of aspect ratios of 4.5-6.5 were found. The results clearly suggest that ω-hydroperfluorohexyl-tails and divalent counterions induce the formation of rod-like reverse micelles in W/CO_2 mixtures, even at high temperatures commensurate with in-reservoir conditions.

41 **Graphical abstract**

42

43

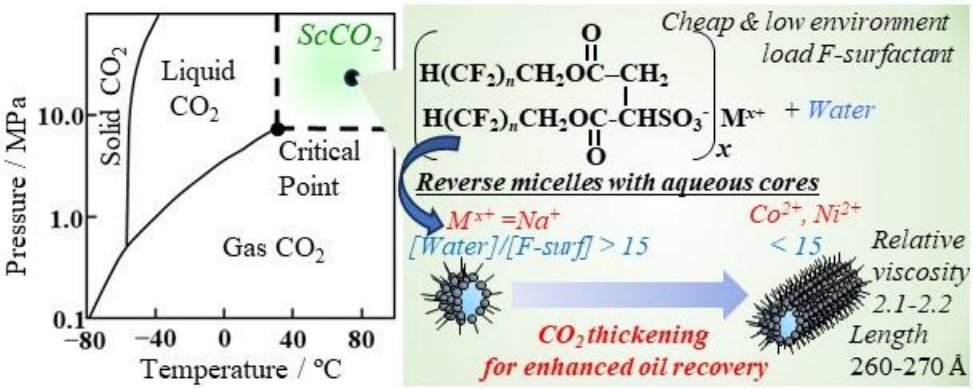

Highlights

- Double ω-hydroperfluorocarbon-tail surfactants were studied in supercritical CO_2 ($scCO_2$)
- Surfactant induced $scCO_2$ thickening was observed at high temperatures commensurate with typical reservoir conditions
- CO_2 viscosity doubled by the surfactant rod-like reverse micelles with lengths of ~260 Å at 75 ºC
- An effective surfactant packing parameter of 1.1-1.8 is required to form rod-like reverse micelles

Keywords

Supercritical CO_2, ω-hydroperfluorocarbon, viscosity, rod-like reverse micelle, Small-Angle Neutron Scattering

1. Introduction

Supercritical CO_2 ($scCO_2$) is a nonpolar solvent with attractive properties such as low cost, inflammability, natural abundance, high mass transfer, and pressure/temperature-tunable solvency (CO_2 density) [1]. For these reasons, it has received much attention as a green solvent for industrial applications like organic synthesis, dry cleaning, polymerization, extraction, nanomaterial processing, and enhanced oil recovery (EOR). However, polar compounds are generally insoluble in $scCO_2$, limiting its use in such industrial applications. For example, EOR with CO_2-flooding (CO_2-EOR), suffers a significant problem that the CO_2 viscosity is notably lower than that of the crude oil to be displaced, leading to inefficient volumetric sweep of the porous media [2,3]. One of the most promising approaches to increase $scCO_2$ viscosity is to generate reverse micelles in the continuous $scCO_2$ phase. If these micelles also contain water in their polar cores, they may be termed water-in-$scCO_2$ microemulsions (W/CO_2 μEs) [3,4]. Such multi-component self-assemblies display not only the attractive characteristics of $scCO_2$, but also the solvation properties of bulk water, and so have potential as volatile organic compound (VOC)-free and energy-efficient solvents for nano-material synthesis, enzymatic reactions, dry-cleaning, dyeing, and preparation of inorganic/organic hybrid materials, amongst other potential applications [5]. For CO_2-EOR processes, the reverse micelles should have a rod-like morphology leading to increased viscosity and thickening of $scCO_2$ [3]. To broaden applications of $scCO_2$ it is of interest to develop highly efficient CO_2-philic surfactants, which will also generate rod-like reverse micelles: this field has been actively researched since the early 1990s [4].

Over the last three decades, there have been continued efforts developing CO_2-philic hydrocarbon surfactants for W/CO_2 μE for economic and environmental reasons [4-8]. In the early 1990s, CO_2-philic materials were explored in commercially available polymers, surfactants, and other oleo-philic substances. However, these were mostly insoluble in $scCO_2$ and therefore inactive for modifying the properties of $scCO_2$ [4]. Aerosol-OT (sodium bis-(2-ethyl-1-hexyl) sulfosuccinate, AOT), widely known as a special surfactant able to stabilize effectively and efficiently water-in-oil (W/O) microemulsions [9], is also insoluble in $scCO_2$ and hence does not stabilize W/CO_2 μEs [4]. Initial investigations clarified that

conventional surfactant-design theory cannot be applied to W/CO_2 systems, and that the concept "CO_2-philicity" is not equivalent to oleo-philicity. Therefore, development of CO_2-philic surfactants has forced new directions and paradigms in the field of surfactant molecular-design. Based on new design principles, tailor-made surfactants for stabilization of W/CO_2 μEs and rod-like reverse micelles in scCO_2 have been introduced [3].

In the earlier studies, certain fluorinated surfactants, including perfluoropolyethers (PFPFs) and fluorinated AOT analogues, were reported to dissolve in scCO_2 and to reduce W/CO_2 interfacial tension, hence implying feasibility for generating W/CO_2 μEs and rod-like reverse micelles [10-13]. This compatibility has been explained in terms of lower surfactant interfacial packing densities and weaker attractive inter-micellar interactions of FCs, which are believed to be beneficial for stabilization of W/CO_2 μEs compared to HCs [10-15]. The water-solubilizing power of these surfactants in CO_2 is often discussed in terms of the water-to-surfactant molar ratio W_0 (=[water]/[surfactant]). Hereafter, the maximum W_0 attainable in a single-phase W/CO_2 μE, namely W_0^{max}, a measure of the solubilizing power of a given surfactant.

With the aim of optimizing CO_2-philic surfactant structure, a range of custom-made double-tail FC AOT analogues were examined [16-20]. The most efficient surfactant from this group was found to be 4FG(EO)$_2$ which, despite having the shortest FC (perfluorobutyl) tails, could stabilize globular W/CO_2 μEs with W_0^{max} = 80 at 75°C [16]. Considering that FC tails are CO_2-philic and longer FC-tail surfactants generally show higher W_0^{max} [16-20], the fact that this high stability occurs with the shortest chain FC 4FG(EO)$_2$ is at first sight surprising. In further studies, the minimum fluorine content necessary to render a surfactant CO_2-philic was examined [21,22], revealing that at least two perfluorethyl groups (CF_3CF_2-) were required to stabilize W/CO_2 μEs. In addition, double-FC-tail phosphate surfactants were found to be efficient μE stabilizers, the most favorable case stabilizing W_0 up to 45 [23,24]. Through these investigations, the effects of FC-tail chemical structure on W/CO_2 μEs stabilization and solubilizing power were revealed, to identify the most efficient FC moieties.

An interesting class of twin-tailed hybrid surfactants, with a separate HC and FC chain have also been evaluated for W/CO_2 μEs [25-29]. For example, sodium 1-pentadecafluoroheptyl-1-octanesulfate (F7H7, $(C_7H_{15})(C_7F_{15})CHOSO_3Na$) gave a high solubilizing power W_0^{max} = 35 [25]. On the other hand, F7H7 analogues with different FC and HC chain lengths, M-F*m*H4 (Counter ions M= Li, Na, and K, perfluorocarbon length *m* = 7 and 8), successfully stabilized W/CO_2 μEs, but with smaller W_0^{max} values than for F7H7 [3,26,27]. A notable finding with this M-F7H4 series was formation of rod-like reverse micelles with M=Na^+, but rather ellipsoidal or spherical with M=Li^+, K^+ or Rb^+. The length and aspect ratio (rod length/diameter) of Na-F7H4 rod-like reverse micelles reached 525 Å and 10.5 respectively at a surfactant concentration of 4.4 wt% (75 mM), W_0 = 12.5, at a pressure of 400 bar and temperature of 40 ºC [3,26,27]: based on the Huggins equation relative viscosities (the ratio of micellar solution viscosity to pure CO_2 viscosity) of ~2 were estimated [30,31]. Such rod-like reverse micelles with high aspect ratios were expected to thicken dense CO_2, as would be required for EOR applications [3].

Recently, using another series of hybrid surfactants, sodium 1-oxo-1-[4-(perfluoroalkyl)phenyl]alkane-2-sulfonates, FC*m*-HC*n* (FC length *m* = 4, 6, HC length *n* = 2, 4, 5, 6 and 8), the effects of FC and HC chain length were examined on phase stability and self-assembly structure with W/CO_2 μEs at 45 °C and 350 bar [17,28,29]. The water solubilization per F-atom is another interesting design concept for ranking new CO_2-philic surfactants. For these hybrid surfactants, the optimal HC-tail and FC-tail lengths were found to be *n* = 4 and *m* = 6 respectively (i.e. FC6-HC4), which stabilized W/CO_2 μEs with W_0^{max} = 80, and a solubilizing power per F-atom of 6.2. These values are equal to the highest performance and effectiveness reported in any W/CO_2 system studied so far [3-29]. The structures of these FC6-HC*n* reverse micelles at W_0 = 20 (D_2O) were determined by high pressure-small angle neutron scattering (HP-SANS) [28] (surfactant concentration of 17 mM, 45 ºC and 350 bar). Micellar shape transitions were observed on increasing HC-tail length only (ellipsoid for *n* = 4 → cylinder for *n* = 5 and 6 → sphere for *n* = 8), and the aspect ratio reached a maximum of 6.3 with HC-tails *n* = 6. For a surfactant concentration 35 mM, the aqueous (D_2O) rod-shaped reverse micellar core length and

aspect ratio for FC6-HC5 were estimated to be ~880 Å and 36, respectively [29]. These micellar dimensions were used to estimate an intrinsic viscosity [η] = 30.9 and a specific viscosity η_{sp} = 2.07 [29].

Hence, the literature indicates that FC surfactants are CO_2-philic, and hence are promising as stabilizers for W/CO_2 μEs. However, FC surfactants, especially with > C7 like perfluorooctanoic acid (PFOA) or perfluorooctane sulfonic acid (PFOS), have significant disadvantages: they are high cost, not biocompatible and are environmental pollutants [32,33]. Therefore, there is quest to find alterative CO_2-philic surfactants which avoid these problems. For example, ω-hydroperfluorocarbons like HCF_2-$(CF_2)_n$-, possessing a dipole moment at the terminal HCF_2-tip: the precursor alcohol needed to synthesize surfactants of this kind, $H(CF_2)_6CH_2OH$ is known to be cheaper (90 dollar / 100g) compared to the more highly fluorinated $F(CF_2)_6CH_2OH$ (440 dollar / 100g). Furthermore, the H-terminated materials safer and more environmentally acceptable due to the weaker hydrophobicity and better degradability compared with F-terminated analogues [32]. Hence, there are benefits in using ω-hydroperfluorocarbons for CO_2-philic surfactant tails [34-39].

Earlier investigations [34-39] found that a class of AOT analogues with ω-hydroperfluorocarbon tails (e.g. sodium bis(1*H*,1*H*,5*H*-octafluoropentyl)-2-sulfosuccinate, Na(di-HCF4)) stabilize W/CO_2 μEs up to $W_0 \leq 30$. The effect of the surfactant counter ion was also examined using a series of M(di-HCF4)$_x$ analogues (counterion M = Na^+ with x = 1, Co^{2+} and x = 2, and Ni^{2+} and x = 2). For these surfactants HP-SANS was used to investigate micellar/microemulsion structure [38,39]. The regular sodium form, Na(di-HCF4) gave rise to spherical reverse micelles, leading to a modest increase in CO_2 viscosity of 10% even at a surfactant concentration of 10 wt%. In contrast, the Co(di-HCF4)$_2$ and Ni(di-HCF4)$_2$ surfactants, at 50 mM W_0 = 10 at 25 ºC and 400 bar, generated rod-like reverse micelles: length 300 Å with Co(di-HCF4)$_2$ and 700 Å for Ni(di-HCF4)$_2$. Because they behave as anisotropic particles these rod-shaped micelles lead to more significant CO_2 viscosity enhancements of 20-90 % at 6-10 wt% [39]. Thus, employing divalent transition metal ions as counterions for CO_2-philic surfactants seems to be an effective approach to addressing the CO_2 viscosity problem. The counterion effect probably originates from a

decrease in critical packing parameter (CPP) due to an increase in hydrophilic group area/volume induced by large counter ions [39].

All of the rod-like reverse micelles introduced above would be very promising as CO_2-thickeners, however, the temperatures are low (≤ 45 ºC) compared with typical reservoir conditions (e.g. ~100 ºC) [40]. The all-important rod-like micelle formation are likely a result of interactions which are expected to weaken with temperature. Therefore, to explore potential practical uses in CO_2-EOR, detailed investigations at temperatures close to reservoir conditions are required.

With the aim of clarifying the performance of double ω-hydroperfluorocarbon-tail surfactants as CO_2-thickeners, this study has examined phase behavior, viscosities, reverse micelle structures and molecular properties (i.e. CPP and area per molecule) of M(di-CF*n*)$_x$ and M(di-HCF*n*)$_x$ in water/supercritical CO_2 mixtures over 35-75 ºC. The surfactants M(di-HCF*n*)$_x$ have different counterions (Na^+, Mg^{2+}, and Ni^{2+}) and double FC tails of only low F-content ($CF_3CF_2CH_2CH_2CH_2$-, di-CF2 series) or ω-hydroperfluorocarbon-tail ($H(CF_2)_4CH_2$– (di-HCF4 series) or $H(CF_2)_6CH_2$– (di-HCF6 series). The findings described here suggest new directions and strategies for developing CO_2–philic surfactants for generating rod-like reverse micelles and CO_2 thickeners.

2. Experimental Section

2.1. Materials

The family of low fluorine-content surfactants studied here are Nickel 1,5-bis[(1H,1H,2H,2H,3H,3H-pentafluoropentyl)oxy]-1,5-dioxobutane-2-sulfonate (Ni(di-CF2)$_2$), Cobalt 1,5-bis[(1H,1H,2H,2H,3H,3H-pentafluoropentyl)oxy]-1,5-dioxobutane-2-sulfonate (Co(di-CF2)$_2$), Nickel 1,5-bis[(1H,1H,5H-octafluoropentyl)oxy]-1,5-dioxobutane-2-sulfonate (Ni(di-HCF4)$_2$), Cobalt 1,5-bis[(1H,1H,5H-octafluoropentyl)oxy]-1,5-dioxobutane-2-sulfonate (Co(di-HCF4)$_2$), Nickel 1,5-bis[(1H,1H,7H-dodecafluoroheptyl)oxy]-1,5-dioxobutane-2-sulfonate (Ni(di-HCF6)$_2$), Cobalt 1,5-bis[(1H,1H,7H-dodecafluoroheptyl)oxy]-1,5-dioxobutane-2-sulfonate (Co(di-HCF6)$_2$), and Sodium 1,5-bis[(1H,1H,7H-dodecafluoroheptyl)oxy]-1,5-dioxobutane-2-sulfonate (Na(di-HCF6)). All the surfactants were synthesized and purified as described in ref [34-39]. Chemical structures of these surfactants are {R-OCO-CH(-SO_3^-)-CH_2-COO-R}$_x$$M^{x+}$, where M^{x+}=Co^{2+}, Ni^{2+}, or Na^+, R=$CF_3CF_2CH_2CH_2CH_2$- for di-CF2, H$(CF_2)_4CH_2$- for di-HCF4, or H$(CF_2)_6CH_2$- for di-HCF6, **Figure S1** in Supplementary data).

Ultrapure water with a resistivity of 18.2 MΩ cm was obtained from a Millipore Milli-Q Plus system. CO_2 was of > 99.995% purity (Taiyo Nippon Sanso Corp.). The structures of the steric models and the length of surfactant molecules (in isolation) were calculated by MM2 (Molecular Mechanics program 2) calculations (Chem 3D; CambridgeSoft Corp., Cambridge, MA).

2.2. Phase behaviour measurements

A high-pressure vessel with an optical window and moveable piston was used to observe phase behavior of the surfactant/water/scCO_2 mixtures with varying pressures and temperatures. A detailed description of the experimental apparatus and procedures for the measurements can be found elsewhere [16-20,28,29].

The measurements of the water/surfactant/scCO_2 systems were performed at temperatures of 35 – 75 °C and pressures < 400 bar. The densities of CO_2 were calculated using the Span-Wagner Equation of

197 state (EOS) [41]. Pre-determined amounts of the surfactant and CO_2 (20.0g), where the molar ratio of
198 surfactant to CO_2 was fixed at 1.92×10^{-3} (i.e. 40 mM at 350 bar and 45 ºC), 0.96×10^{-3} or 3.84×10^{-3}
199 were loaded into the variable-volume high-pressure optical cell, and the appropriate aliquot of water was
200 added through a six-port valve. The surfactant molar concentration varied between 20-40 mM in case of
201 the molar ratio of surfactant to $CO_2 = 1.92\times 10^{-3}$, as the inner volume of the cell was varied by changing
202 experimental pressure and temperature. The physical properties of the continuous phase of $scCO_2$ were
203 assumed to be equivalent to those of pure CO_2.

204

205 **2.3 High-Pressure viscosity measurements**

206 The relative viscosity of the surfactant/water/CO_2 solutions to pure CO_2 was measured with a
207 capillary-type high-pressure viscometer as shown in **Figure S2**. CO_2 high pressure cell, and pressure
208 gauges are the same as in the apparatus for phase behavior measurements. The cell, valves, joints, and all
209 SUS 316 tubes are temperature-controlled with a heater within ±0.5 ºC.

210 According to the Hagen-Poiseuille Equation (1) [42], viscosity is proportional to a differential
211 pressure between inlet and outlet of a capillary tube when a fluid flows through it.

212 Hagen-Poiseuille Equation $\eta = \frac{\pi P r^4 t}{8 v l}$ (1)

213 where η is viscosity, P is differential pressure, r is inner radius of capillary, l is length of capillary, t is
214 time, and v is volume of fluid. After a transparent single phase of the mixture was obtained, using the
215 same procedure as the phase behavior measurements, the valve between two 6-port valves (IDEX Health
216 & Science, Rheodyne 7010) was closed and the fluid was flowed into the capillary (inner diameter: 0.5
217 mm, length: 50 cm) by pumping at a flow rate of 0.658 ml/min with the high-pressure pump (Nihon
218 seimitsu kagaku co., ltd., NRX-01-H). The differential pressure between inlet and outlet of the capillary
219 was then measured with a high line pressure variable reluctance pressure Sensor (Validyne engineering,

DP363). Relative viscosity η_{rel} of a F-surfactant/water/CO_2 solution was calculated by dividing the differential pressure of the surfactant solution by that of pure CO_2 as shown in the following equation.

$$\eta_{rel} = \frac{\eta_{CO2-surf}}{\eta_{CO_2}} = \frac{P_{CO_2-surf}}{P_{CO_2}} \quad (2)$$

Where η_{CO2} is viscosity of pure CO_2, $\eta_{CO2\text{-}surf}$ is viscosity of a water/surfactant/CO_2 system, P_{CO2} is differential pressure for pure CO_2, $P_{CO2\text{-}surf}$ is differential pressure for a water/surfactant/CO_2 solution. All the viscosity measurement was expected to be under laminar flow conditions. For example, the Reynolds number (*Re*) was calculated as ~310 in the case of pure CO_2 at 75 ºC and 350 bar from the equation $Re = Q\,D_H/(vA)$, where Q is the volumetric flow rate, D_H is the hydraulic diameter of the capillary, v is the kinematic viscosity (v = 8.9 x 10^{-8} m^2 s^{-1})[43], A is the capillary's cross-sectional area [44]. Shear rate γ was calculated as 890 s^{-1} from the equation $\gamma = 4Q\,D_H/(\pi r^3)$ [45].

2.4 High-Pressure Small-Angle Neutron Scattering (HP-SANS) measurements and data analysis

Due to the range of neutron wavelengths available, time-of-flight SANS is suitable for studying the shapes and sizes of colloidal systems. High-pressure SANS (HP-SANS) is a particularly important technique for determining aggregate nanostructure in supercritical CO_2. The HP-SANS measurements of the D_2O/scCO_2 systems with di-HCF6 series with Ni, Co, and Na counterions were performed at 45 or 75 °C at various pressures. The LOQ time-of-flight instrument, and the SANS2D instrument, at the Rutherford Appleton Laboratory at ISIS UK, were used in conjunction with a stirred high-pressure cell (Thar). The path length of the cell and neutron beam diameter were both 10 mm. The measurements gave absolute scattering cross sections $I(Q)$ (cm^{-1}) as a function of momentum transfer Q ($Å^{-1}$), which is defined as $Q = (4\pi/\lambda)\sin\theta$, where θ is the scattering angle. The accessible Q ranges were 0.007-0.22 $Å^{-1}$ for LOQ and 0.002-1 $Å^{-1}$ for SANS2D arising from an incident neutron wavelength, λ, of 2.2-10 Å. The data were normalized for transmission, empty cell, solvent background, and pressure induced changes in cell volume as before [28,29].

Pre-determined amounts of D_2O and surfactant, where the molar ratios of surfactant to CO_2 were fixed at 1.92×10^{-3} (= 40 mM at the appropriate experimental condition, respectively), were loaded into the Thar cell. Then, CO_2 (11.3g), was introduced into the cell using a high-pressure pump, and the surfactant/D_2O/CO_2 mixture was pressurized to 350 bar at 45 or 75 ºC by decreasing the inner volume of the cell. With vigorous stirring, visual observations were carried out to identify a transparent single-phase (W/CO_2 μEs). Finally, the HP-SANS experiments were performed for the single-phase W/CO_2 μEs. Due to the systems being dilute dispersions (volume fractions typically 0.12 or less), the physical properties of the continuous phase of scCO_2 were assumed to be equivalent to those of pure CO_2.

Scattering length densities of surfactants, CO_2 and D_2O were calculated (section S3 in supplementary information). The shells of the surfactant/D_2O/CO_2 μEs were estimated to be composed of the fluorinated tails **R** in **Fig. S1**, and the scattering length density (SLD), $\rho_{shell,}$ was calculated as 3.50×10^{10} cm^{-2} for the fluorinated chain $H(CF_2)_6$- from Equation (S1) in supplementary data. On the other hand, aqueous cores with D_2O were suggested to contain the hydrophilic parts of the surfactants, which means the other molecular parts except the fluorinated chain. Then the SLD values of cores, $\rho_{core,}$ were estimated as $4.76\text{-}5.85 \times 10^{10}$ cm^{-2} for Ni and $4.77\text{-}5.86 \times 10^{10}$ cm^{-2} for Co at W_0 = 5-20, and increased with D_2O content, namely W_0. For the SLD calculation of the shell and the cores mass densities of 1H-perfluorohexane, dimethylsuccinate, Nickel sulfonate, and Cobalt sulfonate at 25 ˚C were employed as 1.68 g cm^{-3}, 1.09 g cm^{-3}, 1.80 g cm^{-3}, and 1.77 g cm^{-3}, respectively [46]. As ρ_{shell} was far from ρ_{CO2} (2.29×10^{10} cm^{-2} at 45 ˚C and 2.02×10^{10} cm^{-2} at 75 ˚C), SANS from the D_2O/F-surfactant/CO_2 μEs was assumed to be from both core and shell, the so-called aqueous core/fluorocarbon shell contrast.

For model fitting data analysis, the W/CO_2 μE droplets were treated as spherical, cylindrical or ellipsoidal particles with Schultz distributions in core radius and length [47]. The polydispersities in those radii and lengths were fixed at 0.2 as found in typical W/O μEs [48]. Full accounts of the scattering laws are given elsewhere [36-39,47,49]. To account for weak attractive interactions between microemulsion droplets, square well structure factor ($S(Q)$) was also employed. The perturbation parameter is $\varepsilon = \Delta/(\sigma+\Delta)$, where

Δ and σ are the width of the attractive square well pair potential and the hard core diameter ($\sigma = 2R_c$), respectively. The attractive stickiness, τ, is defined as

$$\tau = \frac{1}{12\varepsilon}\exp(U_0 kT) \qquad (3)$$

τ is a function of both the perturbation parameter and the interaction strength in terms of the depth of the well, U_o. From the definition, that smaller τ means stronger attraction.

Data were fit to the models described above using the SasView small-angle scattering analysis software package (http://www.sasview.org/). The fitted parameters were the core radius $R_{f\text{-}cyl}$ and the length $L_{f\text{-}cyl}$ for core/shell cylindrical particles; these values were initially estimated by preliminary Guinier analyses ($L_{g\text{-}cyl}$, $R_{g\text{-}cyl}$) [29,50]. During the fitting analysis shell thickness was kept constant at 7.4 Å as estimated from the tail structure of $H(CF_2)_6$- by the MM2 simulation.

2.5. Surface pressure measurements

Surface pressure-area isotherms were measured on a KSV minitrough (KSV 2000, KSV Instruments Ltd.) equipped with a platinum Wilhelmy plate, at 35 ºC. In each experiment, a chloroform solution containing surfactant was spread on the water surface. 15 minutes were allowed for solvent evaporation before compression. The barrier was moved at a speed of 10 mm min^{-1}.

3. Results and Discussion

3.1 Effects of counterion, water content, pressure, and fluorinated tail on microemulsion formation

Above a threshold phase boundary pressure (P_{trans}) the surfactant/water/CO_2 mixtures formed transparent single-phases (i.e. Winsor-IV W/CO_2 μE). On the other hand, transparent phase change into a turbid macroemulsion or a precipitated hydrated phase below P_{trans} (i.e. lower CO_2 density). The P_{trans} and the CO_2 density for surfactant/W/CO_2 mixtures were determined for various W_0 values and temperatures (35-75 ºC), as shown in Supplementary data (**Figures S3-S9**). **Figure 1** displays P_{trans} for surfactant/water/CO_2 mixtures with W_0 =10 or 20 at [surfactant]/[CO_2]=1.92×10^{-3}. In this Figure, 1ϕ and 2ϕ represent transparent single-phase and two-phase systems, respectively. Some of these surfactants at [surfactant]/[CO_2]=1.92×10^{-3} were not completely dissolved in CO_2 at any pressure and temperature studied. For example, the mixtures for Co(di-CF2)$_2$ at $W_0 > 5$, Co(di-HCF4)$_2$ at $W_0 > 15$, and Ni(di-HCF4)$_2$ at $W_0 > 10$ were always two-phase under the experimental conditions studied.

Comparing surfactants with the same counterion, it is clear that longer fluorinated tails lead to lower P_{trans}. This may be attributed to increased CO_2-philicity of surfactants bearing longer fluorinated tails, allowing for increased CO_2 solvation and stabilization of microemulsions at lower pressures P_{trans} [16-22]. Looking at surfactants with the same CO_2-philic tails, surfactants can likely form a single phase at lower pressures with smaller atomic number counterions (Na < Co < Ni) or stronger ionization tendency (Na > Co > Ni). This trend may be linked to lower W/CO_2 interfacial tensions, higher counterion dissociation and/or higher hydrogen bonding efficiency with the water of the headgroups [3,26,27,38,39].

In most cases, P_{trans} tends to increase with temperature. However, as indicated by **Figures S3-S9** the phase boundary instability is better thought of in terms of CO_2 density rather than P_{trans}. This has been reported in earlier studies [16-22], and was attributed to solubility in scCO_2 which is a linear function of CO_2 density, rather than pressure [16-22].

On the other hand, as shown in **Figure S3-S9** P_{trans} increases with W_0 for all the surfactants studied. Increasing the water loading induces droplet growth, which may lead to stronger inter-droplet interaction. Hence higher pressures (or CO_2 density) are required to solvate reverse microemulsion droplets with more

313 CO_2 molecules (i.e. a higher CO_2 density or pressure), to prevent aggregation and fusion. As shown in
314 **Figures S10** and **S11** the effect of surfactant concentration on P_{trans} at W_0 =10 was also examined:
315 doubling concentration increases P_{trans} by 6-73 bar. Increasing the surfactant and water concentration
316 together (i,e. at fixed W_0) may be expected to increase attractive interactions, which would destabilize the
317 microemulsions.
318

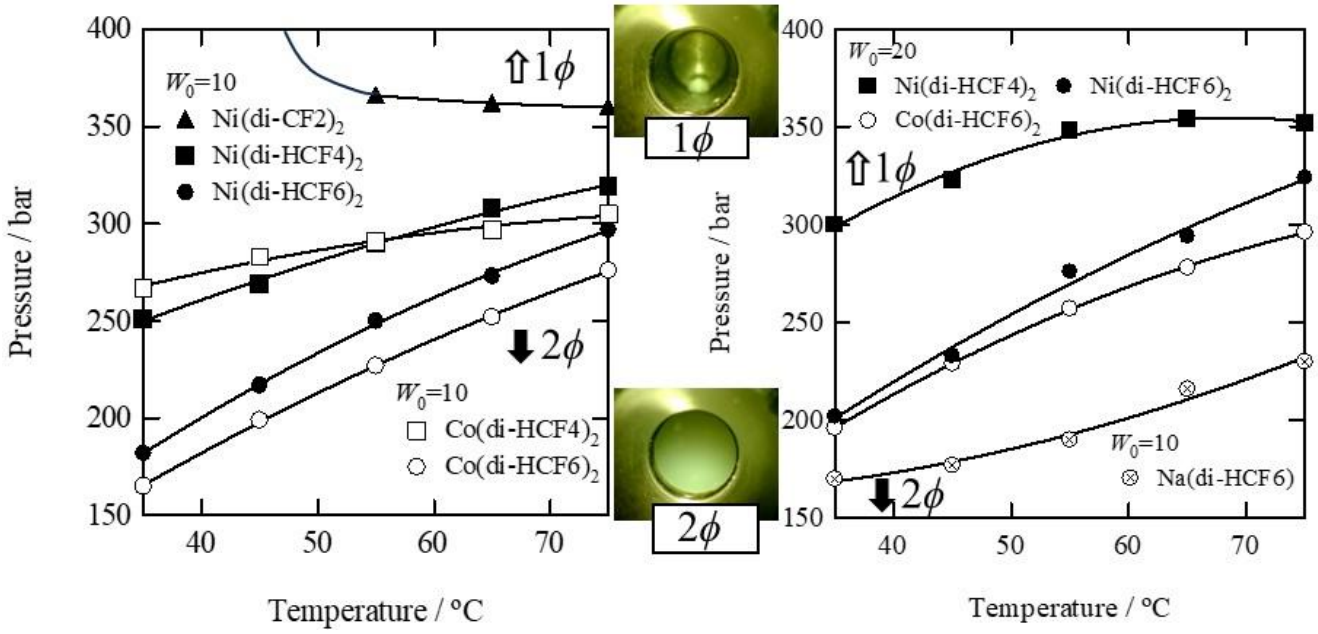

Figure 1. Phase boundary pressures between transparent "micro"emulsion (1ϕ) and turbid "macro"emulsion (2ϕ) systems as a function of temperature for surfactant/W/CO_2 mixtures with W_0 = 10 and 20 and [surfactant]/[CO_2] of 1.92 × 10^{-3} (Co^{2+} and Ni^{2+}) and 3.84 × 10^{-3} (Na^+). Photographs show appearance of 1ϕ and 2ϕ systems, under stirring, in the high-pressure cell.

3.2 Viscosity enhancement of CO_2 by low fluorine-content surfactants

To examine the ability of these surfactant/W/CO_2 systems to increase the viscosity and thicken CO_2, the relative viscosities η_{rel} were measured at 350 bar (**Figures S12-S14**). **Figure 2** shows η_{rel} for systems at W_0=10. To compare the data at the same surfactant anion concentration, [surfactant]/[CO_2] was 3.84×10^{-3} for Na^+, but 1.92×10^{-3} for Co^{2+} and Ni^{2+}. [The measurement of η_{rel} with M(di-CF2)$_2$ W_0=10 was not possible in this rig, since P_{trans} > 350 bar.]

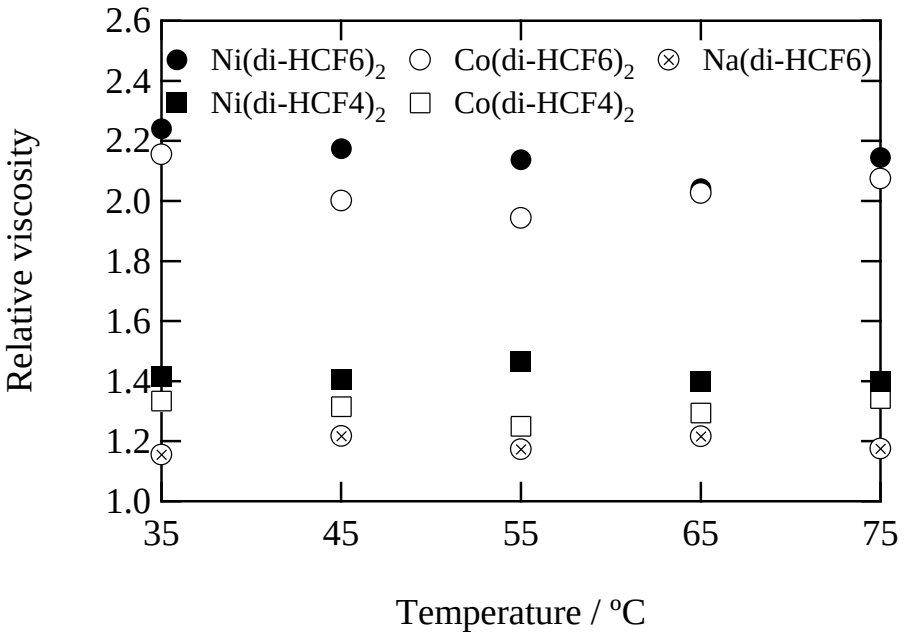

Figure 2 Relative viscosity η_{rel} as a function of temperature for M(di-HCFn)$_x$ (n = 4 or 6, M = Na^+, Co^{2+} or Ni^{2+})/W/CO_2 mixtures with W_0 =10 at 350 bar. The ratios [surfactant]/[CO_2] were 3.84×10^{-3} for Na^+, and 1.92×10^{-3} for Co^{2+} and Ni^{2+}. Shear rates were in the 10-1000 s^{-1} range.

Over the range 35-75 ºC temperature has only a marginal effect on η_{rel}. Longer tail fluorinated surfactants Ni(di-HCF6)$_2$ and Co(di-HCF6)$_2$ gave η_{rel} 1.94-2.24, notably higher than 1.5 for the shorter F-tail analogues Ni(di-HCF4)$_2$ and Co(di-HCF4)$_2$. Surfactants with Ni^{2+} counterions gave higher η_{rel} compared those with to Co^{2+}. It is interesting to note that the Na^+ for the longer fluorinated tails became very low by exchanging the divalent counterion Ni or Co for the monovalent Na-HCF6 gave the lowest η_{rel} values. These results indicate that long fluorinated tails ≥ C_6 and divalent counterions are important feature of these surfactants for CO_2-thickening. A plausible explanation for this chemically specific behavior is that anisotropic, rod-shaped micelles might be formed in the Ni(di-HCF6)$_2$ and Co(di-HCF6)$_2$ systems. Section 3.3 below details structural studies of the micelles/microemulsions in these systems using SANS.

Figure 3 shows the variation of η_{rel} for surfactant/water/CO_2 mixtures as a function of W_0 at 75 ºC and 350 bar. On increasing W_0 up to 10, η_{rel} was found to increase especially for the longer tail surfactants. On the other hand, the η_{rel} gradually decreased for systems at $W_0 > 10$. One possible explanation for these trends is that reverse micelle self-assembly structure changes from spherical to rod-like as a function of W_0, with maximum anisotropy, and hence viscosity occurring about $W_0 \sim 10$. In earlier studies with hybrid H-F surfactants, long rod-like reverse micelles with lengths of > 250 Å were only formed in scCO_2 at W_0 ~10 [29]. Under those conditions the H-F hybrid surfactants reached an effective packing parameter (EPP) of 1.4-1.7, consistent with stabilization for rod-like micelles. Further, the presence of cylinder (rod) micelles was confirmed by SANS [27,38,39].

The effect of surfactant concentration ([surf]) at constant $W_0 = 10$ on η_{rel} in **Figure S14**. For all surfactants and experimental conditions tested, η_{rel} clearly increased with [surf], with the effects being greater for the longer F-chain surfactants M(di-HCF6)$_2$. This would be consistent with longer rod-like micelles with the M(di-HCF6)$_2$ series compared to M(di-HCF4)$_2$ analogues.

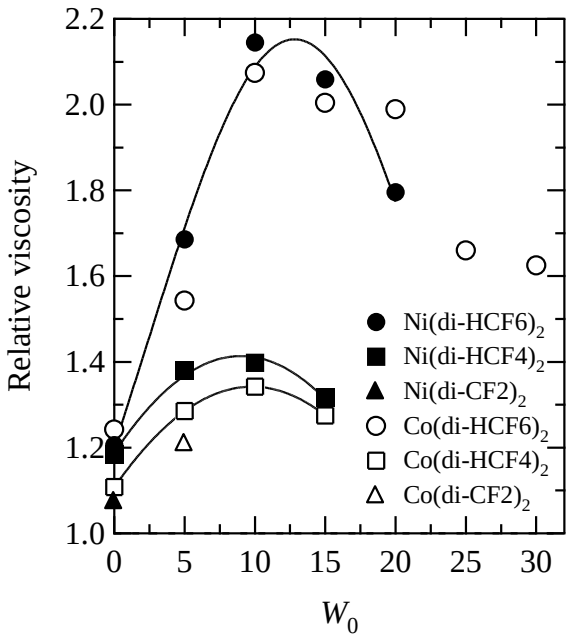

363

364 **Figure 3** Relative viscosities as a function of W_0 for surfactant/W/CO_2 mixtures at 75 ºC and 350 bar. The

365 ratio of [surfactant]/[CO_2] was fixed at 1.92×10^{-3}. Shear rates were in the 10-1000 s^{-1} range.

366

3.3 Structural studies by High Pressure SANS

SANS $I(Q)$ profiles were measured for water/CO_2 μEs at [surfactant]/[CO_2] of 1.92×10^{-3}, 350 bar, 45 and 75 ºC, and different W_0 values. For Ni(di-HCF6)$_2$ and Co(di-HCF6)$_2$ SANS profiles at 75 ºC and 350 bar are shown in **Figure 4.** The SANS data for Na(di-HCF6) at 75 ºC and 350 bar and Co(di-HCF6)$_2$ at 45 ºC and 350 bar can be found in **Figures S19-S20** (Supplementary data).

In the low Q region (typically in the case of droplet μEs < 0.01 Å^{-1}), the SANS may scale as $I(Q) \sim Q^{-D}$, where D is a characteristic "fractal dimension"; hence, the gradient of a log-log plot will be $-D$. In the case of non-interacting spheres, D should be zero in this low Q region, whereas D = 1 for cylinders and 2 for disks [29,49,50]. When viewed in this way, the SANS profiles for Co(di-HCF6)$_2$ and Ni(di-HCF6)$_2$ show D = 1, and 2 for Na(di-HCF6), suggesting the presence of rod-like and disk-like particles, respectively. Using appropriate Guinier plots, the radius of gyration R_g, cylinder radius (or disk radius) $R_{g\text{-}cyl}$ and length (or disk thickness) $L_{g\text{-}cyl}$, sphere radius $R_{g\text{-}sph}$ of water/CO_2 μEs can be estimated (**Figures S15-S18**) and are listed in **Table S1**.

These SANS data were analyzed in detail by model fitting to various form factor models ($P(Q)$) to gain information on the size and morphology of the reverse micelles/microemulsion. As initially indicated based on the logarithmic scaling (Q^{-1} or Q^{-2}), most SANS profiles for these W/CO_2 microemulsions were best-fitted by a form factor for anisotropic particles (which reports on cylinders for aspect ratio ($L_{f\text{-}cyl}/(2R_{f\text{-}cyl}) >> 1$, and disks with ($L_{f\text{-}cyl}/(2R_{f\text{-}cyl}) < 1$). It was found that a small contribution from *S(Q)*, based on a square-well potential, accounting for additional weak attractions, helped improve the fit quality in the low Q regions. The initial values of $R_{g\text{-}cyl}$ and $L_{g\text{-}cyl}$ obtained by trail Guinier plot analyses (**Figures S15-S18, Table S1**) were used as the starting points for the curve fitting. In **Figure 4** the solid lines are the best fitted functions for the cylinder *P(Q)* with a polydispersity index of 0.2 and the *S(Q))* data. The values of $R_{f\text{-}cyl}$ and $L_{f\text{-}cyl}$ are given in **Table 1** and **Table S2** (Supplementary data). In the case of the W/CO_2 mixture with Co(di-HCF6)$_2$ at W_0=20 and 75 ºC, the aspect ratio $L_{f\text{-}cyl}/(2R_{f\text{-}cyl})$ was ~1, suggesting spherical particles. The SANS data was also well-fitted with the theoretical curve of spherical particles with radius of 19.6 Å as shown in supplementary data (Fig. **S21**).

Table 1 Fit parameters obtained from model fitting of SANS profiles for M(di-HCF6)$_x$/water/CO_2 reverse micelles/microemulsions. Radius ($R_{f\text{-}cyl}$) and length ($L_{f\text{-}cyl}$) for cylinder particle *P(Q)*; volume fraction (ϕ); aspect ratio ($L_{f\text{-}cyl}/(2R_{f\text{-}cyl})$; micelle concentration (C_{agg}); aggregation number (N_{agg}); effective water/CO_2 interfacial area ($A_{W/C}$). Also given is the effective packing parameter (EPP) for surfactant molecules. The values of C_{agg}, N_{agg}, $A_{W/C}$, and EPP were estimated from Equations (5)-(10) using $R_{f\text{-}cyl}$, $L_{f\text{-}cyl}$, and ϕ. The value of [surfactant]/[CO_2] was 1.92×10^{-3} for all surfactant systems except Na(di-HCF6), except for Na(di-HCF6) which was 3.84×10^{-3}.

M^{x+}	T / ºC	W_0	$R_{f\text{-}cyl}$ / Å	$L_{f\text{-}cyl}$ / Å	$L_{f\text{-}cyl}/(2R_{f\text{-}cyl})$	ϕ	C_{agg} / (mM)	N_{agg}	$A_{W/C}$ / Å^2	*EPP*
Co^{2+}	75	5	13.8 ± 0.3	238 ± 20	5.95	0.048	0.22 ± 0.03	180 ± 23	121 ± 28	1.32 ± 0.15
		10	23.3 ± 0.1	266 ± 9	4.58	0.051	0.08 ± 0.00	483 ± 22	88 ± 7	1.20 ± 0.05
		15	24.8 ± 0.2	264 ± 9	4.33	0.055	0.09 ± 0.00	465 ± 21	97 ± 8	1.19 ± 0.05
		20	17.8 ± 1.0	37 ± 5	1.03	0.059	1.36 ± 0.34	29 ± 7	208 ± 87	1.47 ± 0.25
	45	5	18.9 ± 0.1	123 ± 2	2.62	0.048	0.23 ± 0.01	174 ± 5	97 ± 5	1.29 ± 0.03
		10	22.9 ± 0.1	194 ± 3	3.45	0.051	0.12 ± 0.00	339 ± 7	92 ± 4	1.22 ± 0.02
Ni^{2+}	75	5	13.6 ± 0.3	92 ± 4	2.54	0.048	0.60 ± 0.05	67 ± 5	134 ± 19	1.42 ± 0.09
		10	14.4 ± 0.1	267 ± 20	6.47	0.051	0.22 ± 0.02	185 ± 16	138 ± 22	1.30 ± 0.11
		15	12.6 ± 0.2	76 ± 3	2.27	0.055	1.15 ± 0.08	35 ± 2	202 ± 24	1.46 ± 0.08
		20	18.9 ± 1.4	24 ± 4	0.74 (Disc)	0.059	1.81 ± 0.58	22 ± 7	233 ± 123	1.52 ± 0.32
Na^{+}	75	5	10.9 ± 0.1	10.1 ± 0.1	0.68 (Disc)	0.052	10.4 ± 0.29	8 ± 0	186 ± 8	2.11 ± 0.04
		10	15.5 ± 0.3	22.0 ± 0.6	0.80 (Disc)	0.059	3.09 ± 0.22	26 ± 2	141 ± 17	1.63 ± 0.08
		15	21.9 ± 0.2	18.9 ± 0.1	0.58 (Disc)	0.067	1.10 ± 0.03	73 ± 2	78 ± 3	1.50 ± 0.02

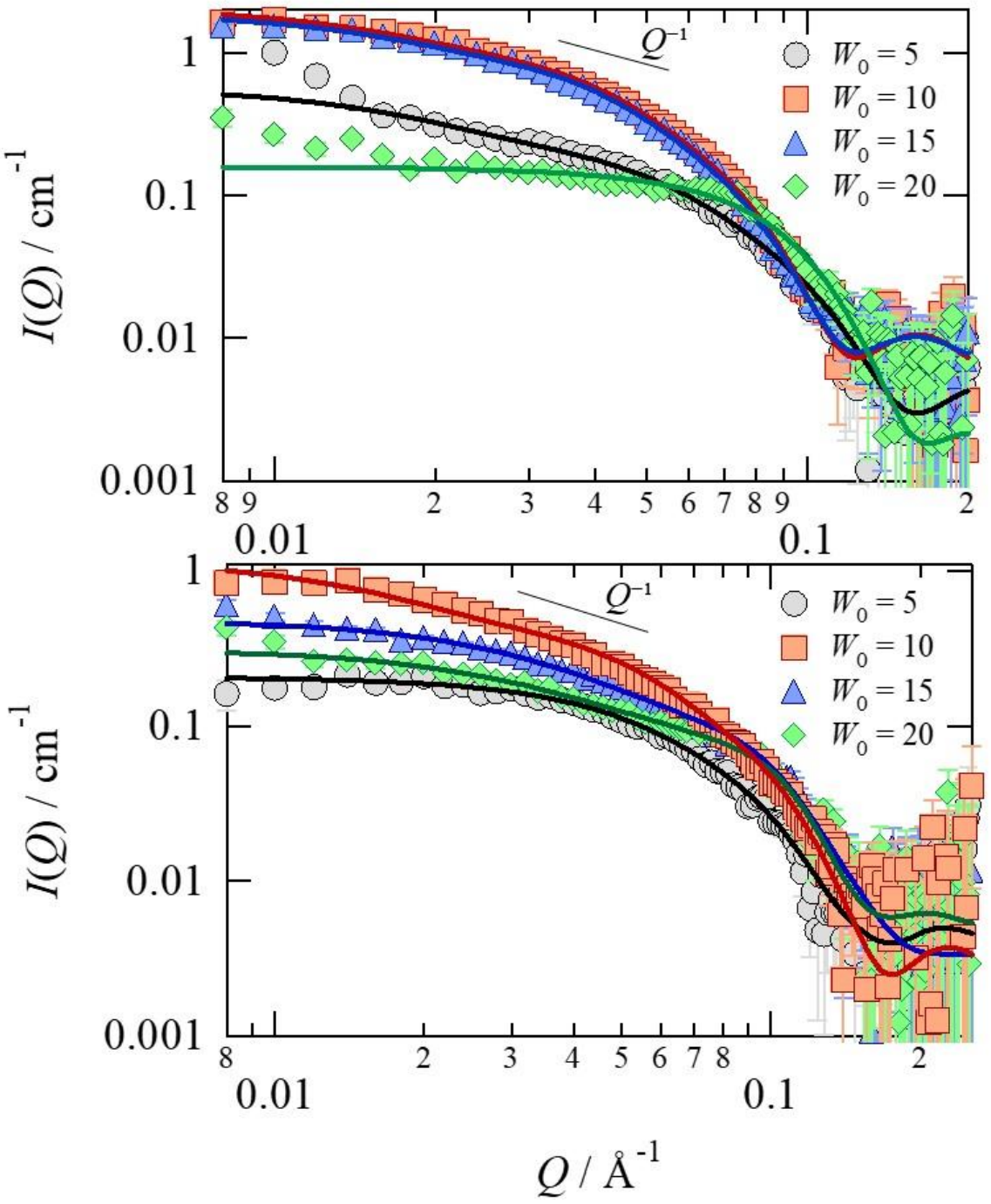

403

404 **Figure 4.** SANS profiles for M(di-HCF6)$_2$/D_2O/CO_2 mixtures with different W_0 values at 75 ºC and 350

405 bar. The ratio [surfactant]/[CO_2] was fixed at 1.92×10^{-3}.The counterion M is (top) Co^{2+} or (bottom) Ni^{2+}.

406 Fitted curves were based on a model incorporating a Schultz distribution of polydisperse cylinder particles

407 with core (D_2O and the hydrophilic group) and a shell (fluorinated tails). A contribution from the square-

408 well structure factor S(Q) was also included in the model.

Visual phase behavior observations as a function of P, T and W_0, showed transparent single-phases above the phase boundary pressures P_{trans}, consistent with W/CO_2 microemulsion phases. However, there is a possibility that small amounts of water separated from the reverse micelle/CO_2 systems, which are difficult to observe by the naked eye. For both surfactants in **Figure 4**, the measured $I(Q)$ profiles at W_0=15-20 were lower than those at W_0=10. This would be consistent with formation of Winsor-II phases (namely a W/CO_2 microemulsion having a separated excess water) at these higher W_0 values (or partially formed a W/CO_2 reverse-type liquid crystal [19,20]). To clarify whether reverse micelles grew regularly with increasing W_0, the ratio of volume-to-surface area (v_{core}/s_{core}) of aqueous core was calculated using $R_{f\text{-}cyl}$ and $L_{f\text{-}cyl}$, and plotted as a function of W_0 (**Figure S22)**. In previous study [28,29], with a strong surfactant such as the FC-HC hybrid FC6-HC4, this value v_{core}/s_{core} tends to increase with W_0, consistent with the formation of Winsor-IV microemulsions (i.e., all the added water is dispersed, with no excess water phase as for a Winsor-II system). In the case of Winsor-IV systems Equation (4) applies,

$$\alpha(p)\,(v_{core}/s_{core}) = (v_{head}\,N_{agg} + v_w\,W_0\,N_{agg}) / (A\,N_{agg}) = (v_{head}/A) + (v_w/A)\,W_0 \qquad (4)$$

where $\alpha(p) = 1 + 2p^2$, p is polydispersity index, v_w is the volume of water molecule, N_{agg} is the aggregation number, v_{head} is the volume of surfactant headgroup and A is the area per surfactant molecule. The values of s_{core} and v_{core} were calculated using $s_{core} = 2\pi R_{f\text{-}cyl} L_{f\text{-}cyl} + 2\pi R_{f\text{-}cyl}^2$ and $v_{core} = \pi R_{f\text{-}cyl}^2 L_{f\text{-}cyl}$ for cylindrical particles. Referring to **Figure S22**, the surfactants Co(di-HCF6)$_2$ and Ni(di-HCF6)$_2$ did not show any significant increase in v_{core}/s_{core} above W_0 = 10. This would be consistent the additional water added above W_0 = 10 not being taken up into reverse micelles, and Winsor-II systems (or W/CO_2 reverse-type liquid crystals [17-20]). The presence of shoulders in the SANS profiles at W_0=20, which are indicated by arrows in **Figure S23**, may be interpreted as Bragg-type peaks, owing to liquid crystalline ordering. SANS profiles for D_2O/CO_2 microemulsions with Co(di-HCF6)$_2$ and Ni(di-HCF6)$_2$ at W_0 = 20, 75 ºC and 350 bar were found to show such Bragg peaks (as pointed by arrows in **Figure S23**). Di-chain surfactants with single head group, structurally akin to lipids [51,52] are known to form liquid crystals: for example, and

436 not limited to, fluorinated double-tail surfactants such as di-HCF6 are found to form lamellar liquid
437 crystals in W/CO_2 mixtures with high W_0 values of > 10 [17-20]. Based on these possible Bragg peaks
438 the layer spacings were estimated as 85 Å for Co(di-HCF6)$_2$ and 68 Å for Ni(di-HCF6)$_2$. Based on the
439 assumption that the hydrophobic tails are 7.4 Å (length of H(CF_2)$_6$- chain), this suggests layers of water
440 + hydrophilic groups to be ~70 Å for Co(di-HCF6)$_2$ and ~53 Å for Ni(di-HCF6)$_2$. These thicknesses
441 would be consistent with electrostatic repulsion between charged head groups and neighboring
442 counterions on opposing surfaces.
443 For W_0 values of 5-10 the surfactants with divalent counterions with Co(di-HCF6)$_2$ and Ni(di-HCF6) gave
444 rise to the greatest anisotropy and micellar elongation, in terms of the aspect ratio ($L_{f\text{-}cyl}/(2R_{f\text{-}cyl})$). In more
445 detail, the micellar morphology of these two surfactants evolved from short rods at W_0=5, to much longer
446 rods at W_0=10, decaying to short rods at W_0=15, and then spheres or oblates at W_0=20. These changes in
447 micellar structure, with long rods at W_0=10, map on to the η_{rel} behavior seen in **Figures 2** and **3**. Finally,
448 formation of the longest rod-like reverse micelles $L_{f\text{-}cyl}$ ~260 Å lead to η_{rel} ~ 2. This represents the first
449 observation of rod-like reverse micelles in CO_2 at a temperature of 75 ºC, which is close to real reservoir
450 conditions. To explore further how to control reverse micelle morphology, to generate the longest rods
451 (worm-like or thread-like ones), the next section considers the effects of counterion, W_0, and surfactant
452 concentration on aggregation number (N_{agg}) and effective packing parameter (EPP).
453

3.4 Micellar structure and surfactant architecture

To investigate the aggregation properties of these surfactants in $scCO_2$, the aggregation number (N_{agg}) and area occupied per molecule at the W/CO_2 μE surface ($A_{C/W}$) were calculated via the following Equations [29,53].

$$N_{agg} = C_{surf}/C_{agg} \quad (5)$$

$$A_{C/W} = s_{core}/N_{agg} \quad (6)$$

$$C_{agg} = (V_{D2O}\, C_{D2O} + V_{head}\, C_{surf})/(V_{core}) = C_{surf}\, (V_{D2O}\, W_0 + v_{head}\, N_A)/(v_{core}\, N_A) \quad (7)$$

where C_{surf}, C_{agg} and C_{D2O} are molar concentrations of surfactant, micelle, and D_2O, respectively. N_A is the Avogadro number, V_{D2O}, V_{head}, and V_{core} are molar volumes of D_2O, surfactant headgroup and aqueous core, v_{core} and v_{head} are volumes per aqueous core ($V_{core} = v_{core}\, N_A$) and headgroup ($V_{head} = v_{head}\, N_A$), respectively. The values of v_{head} are shown in the section **S2** in Supplementary data. The assumption implicit in these calculations is that all surfactant molecules are adsorbed at the W/CO_2 interface. In real W/CO_2 microemulsions, it is likely that a small fraction of the surfactant molecules will partition away from the interface owing to low background solubilities in water and CO_2. However, this is estimated to be negligible compared with total number of associated surfactant molecules (9.6×10^{-2} mol%), taking into account only very low critical microemulsion concentrations in $scCO_2$ for ionic F-surfactants, typically < 10^{-4} mol % [3,20,26-29,38,39,54,55]. The values of C_{agg}, N_{agg}, and $A_{C/W}$ are listed in **Table 1**, and changes in N_{agg} as a function of W_0 are displayed in **Figure S25**. The figures also include data for W/CO_2 microemulsions with the hybrid surfactant M-F7H4 (M=Li^+, K^+, Na^+) [3,26,27], FC6-HC*n* [28,29], double-tail surfactants *n*FG$(EO)_2$ (*n* = 4 and 8) [20], Ni(di-HCF4)$_2$ [38,39], and regular W/O microemulsions with AOT in *n*-heptane [54]. The broken circle in the plot indicates conditions at which long rod-like reverse micelles with length > 250 Å formed.

As expected, owing to growth and elongation of reverse micelles/microemulsion droplets with increasing W_0, the N_{agg} values increase with W_0 as shown in **Figure S25**. Such an increasing trend of N_{agg} with W_0 was also reported in the different W/CO_2 and W/O microemulsions stabilized by other surfactants [3,20,26-29,38,39,54,55]. The gradient becomes steeper for rod-like reverse micelles (see the broken

480 circle for the long rod-like reverse micelle region). On the other hand, for Co(di-HCF6)$_2$ and Ni(di-
481 HCF6)$_2$, N_{agg} drastically decreases as the micelle morphology evolves from rod-like to globular in the
482 single phase Winsor-IV systems at $W_0 = 10$, and then into two-phase Winsor-II or co-existing liquid crystal
483 systems at $W_0 \geq 15$ (**Table 1)**.

484 N_{agg} values decrease in the order of $Na^+ < Ni^{2+} < Co^{2+}$. Regarding $A_{W/C}$ the value for Co^{2+} was the
485 lowest, perhaps owing to stronger interactions between Co^{2+} ions with the -SO_3^- headgroups leading to
486 greater electrostatic shielding of -SO_3^- - -SO_3^- repulsions. Similarly, at the air/water interface and 35 ºC
487 the effective area per surfactant anion for Co(di-HCF6)$_2$ was also lower compared with that for Ni(di-
488 HCF6)$_2$ (**Figure S24** and **Table S3**). In addition, the $A_{C/W}$ values for Co^{2+} and Ni^{2+} ions were less than
489 double those for Na^+ although the divalent-ion analogues have two surfactant ions per molecule. It
490 suggests that the larger $A_{C/W}$ values for Na^+ ion does not arise principally owing to steric hindrance
491 between the fluorinated tails solvated with CO_2, but rather stronger -SO_3^- - -SO_3^- electrostatic headgroup
492 interactions and weaker screening by Na^+ ions. Interestingly, the $A_{C/W}$ values for Na(di-HCF6) are quite
493 close to those of other the double F-tail anionic surfactants with Na^+ counterions, (*n*FG(EO)$_2$ and
494 *n*FS(EO)$_2$) as mentioned above [16,20,49].

495 Generation of rod-like reverse micelles could be accounted for by changes in critical packing
496 parameter (CPP) (i.e. spontaneous packing parameter, SPP) and/or hydrophilic-CO_2-philic balance (HCB).
497 These packing indices can be thought of as a measure of the molar Gibbs free energy difference ($\Delta\bar{G}$
498 $_{sphere \rightarrow cylinder}$) [56] between the endcaps (i.e. semi-spheres) and the cylindrical body of rod-like reverse
499 micelles. Based on this concept, the Co^{2+}surfactant would generate a more negative $\Delta\bar{G}_{sphere \rightarrow cylinder}$ (= $\bar{G}$
500 $_{cyl\text{-}body} - \bar{G}_{endcap}$), implying that the surfactant molecules prefer cylindrical, rather than endcap packing.
501 According to theory [57-59] SPP can be obtained by

502 $$SPP = v_{tail}/(A_0\, l_{tail}) \qquad (8)$$

where v_{tail} and l_{tail} are hydrophobic tail volume and length, respectively (the same meanings as in the expression for [59]). Entropy is taken into account by the fact that the preferred area per molecule A_0 minimizes the free energy of the surfactant film. According to this approach, reverse micelles would be obtained with SPP > 1 (reversed cores form if the surfactant tails orient upward) to ~1 (cylindrical). In the case of W/CO_2 microemulsions, the A_0 and v_{tail} values used to generate EPP should be calculated taking into account solvation of the head and tail groups with water and CO_2. If the hydrophobic part is assumed to be a truncated cone, the volume would be [29,53]

$$v_{tail} = l_{tail}\{A_{C/W} + A_{tail} + (A_{C/W}\, A_{tail})^{0.5}\}/3 \qquad (9)$$

where A_{tail} is area per hydrophobic tail terminus, respectively. For the calculation of EPP in W/CO_2 microemulsions, when A_0 is replaced by $A_{C/W}$, Eq. (8) can be simply expressed as

$$\text{EPP} = \{s_{agg} + s_{core} + (s_{agg}\, s_{core})^{0.5}\}/(3s_{core}) \qquad (10)$$

where s_{agg} is surface area per reverse micelle. The values of s_{agg} were calculated from the cylindrical core length and radius ($L_{f\text{-}cyl}$ and $R_{f\text{-}cyl}$) fitted to the SANS data, and assuming 7.4 Å for the surfactant tail length l_{tail} [16-20]. The calculated EPP values are listed in **Table 1** and plotted as a function of W_0 at different surfactant concentrations in **Figure 5** (or **Figure S26**).

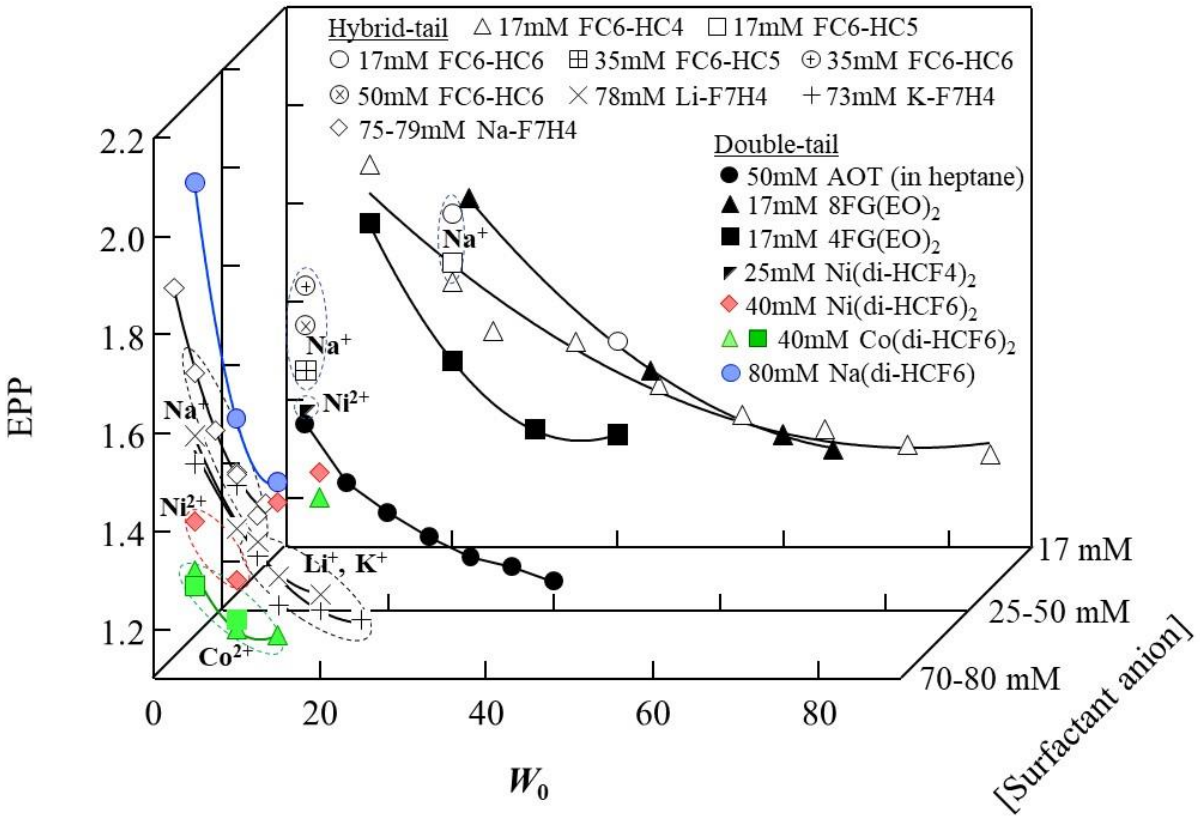

520

521 **Figure 5.** Changes in effective packing parameter EPP for reverse micelles as a function of W_0 for
522 D_2O/CO_2 μEs with hybrid and double-tail surfactants or D_2O/*n*-heptane μEs stabilized by normal AOT
523 [3,20,26-29,38,39,53]. Experimental conditions were 45 °C and 350 bar for 17mM FC6-HC*n* (*n* = 4-6)
524 and 17mM *n*FG(EO)$_2$ (*n* = 4, 8), 23-40 ºC and 380-400 bar for 78 mM Li-F7H4 and 73 mM K-F7H4, 75-
525 79 mM Na-F7H4, 25 ºC and 350-400 bar for 25 mM Ni(di-HCF4)$_2$, 45 ºC or 75 ºC and 350 bar for 40
526 mM M(di-HCF6)$_2$ (M=Co and Ni) in D_2O/CO_2 μEs, 75 ºC and 350 bar for 80 mM Na(di-HCF6) in
527 H_2O/CO_2 μEs, and 25 °C and 1 bar for 50 mM AOT in D_2O/*n*-heptane μEs. The broken circles indicate
528 formation of rod-like reverse micelles with aspect ratios ($=L_{f\text{-}cyl}/(2R_{cyl})$) > 2.5 for each counterion.

529

Similar to earlier reports [3,20,26-29,38,39,54], EPP values for the di-HCF6 series decreased with increasing W_0, consistent with decreases in negative curvature of reverse micelles.

Comparing EPP values for all these surfactants, rates of decrease in EPP vs W_0 tend to be steeper with increasing surfactant-ion concentration from 17 mM to 80 mM. On the other hand, divalent counterions Ni^{2+} and Co^{2+} gave rise to lower EPP values compared with monovalent ions Li^+, Na^+, and K^+ at the same W_0 values. Comparing Co^{2+} with Ni^{2+} the EPP values for Co^{2+} are smaller, which would fit with the explanation given above for changes in $A_{C/W}$, based on the strength of interactions between $-SO_3^-$ headgroups and the two different counterions.

The broken circles in **Figure 5** indicate formation of rod-like reverse micelles with aspect ratios > 2.5. From the locations of the broken circles, rod-like reverse micelles appear at W_0 = 5-20 corresponding to EPP values in the range 1.1-1.8. **Figure 5** also shows that surfactant-ion concentration also plays an important role in generating elongated reverse micelles: the higher the surfactant-ion concentration, the higher the tendency to form rod-like reverse micelles. It is probably due to shortening of the intermicellar distance, which in turn increases the strength of the intermicellar interactions. From these results and discussion, under appropriate EPP, surfactant concentration and W_0 conditions, as well as employing divalent Co^{2+} or Ni^{2+} counterions rod-like reverse micelles can be generated in W/CO_2 systems.

4. Conclusions

Dense CO_2 fluids containing reverse micelles with aqueous cores represent interest in, and potentially useful, media for applications such as extraction, dyeing, dry cleaning, enzymatic reaction, and organic/inorganic or nanomaterial synthesis [5]. Regarding enhanced oil recovery using CO_2-flooding, rod-like or worm-like reverse micelles are able to significantly thicken CO_2, improving the currently poor sweep efficiency by preventing fingering phenomenon in reservoirs [2,3]. Previous studies [29] found the hybrid surfactant FC6-HC5 to form rod-like reverse micelles with a length of ~880 Å in W/supercritical CO_2 mixtures at 350 bar and 45 ºC. It was estimated that these long and thin micelles would lead to a factor of three increase in CO_2 viscosity: compared to earlier surfactant/W/CO_2 systems [3-13,16-29,34-39] that represents the largest viscosity enhancement of CO_2. Unfortunately, owing to cost and bioaccumulation, these hybrid H-F surfactants are less appropriate for practical applications. On the other hand, it has been shown that low F-content double tail ω-hydroperfluorocarbon anionic surfactants with various counterions Na(di-HCF4), Co(di-HCF4)$_2$ and Ni(di-HCF4)$_2$, generate rod-like reverse micelles with lengths of 200-700 Å in liquid CO_2 at 25 ºC [38,39]. Although this is very promising for practical uses in EOR, further investigations at higher temperatures, close to reservoir conditions of ~100 ºC were needed.

This new study investigated the formation of rod-like reverse micelles in supercritical CO_2 under high temperature (75 ºC) and pressure 350 bar conditions. The series of surfactants studied here are AOT-like anionic surfactants with different counterions (Na^+, Co^{2+}, and Ni^{2+}) and a double CO_2-philic tail with low F-content (di-CF2 series) or ω-hydroperfluorocarbon-type (di-HCF4 and di-HCF6 series), which are more inexpensive, biocompatible and environmentally-benign. Phase behavior observations, viscosity measurements and SANS experiments at [surfactant]/[CO_2] = 0.96×10^{-3}, 1.92×10^{-3}, or 3.84×10^{-3} revealed new findings (1)-(5) as shown below,

(1) Cylindrical micelles formed by double ω-hydroperfluorohexyl(C_6)-tail surfactants Ni(di-HCF6)$_2$ and Co(di-HCF6)$_2$ were able to enhance CO_2 viscosity by factors of 1.94-2.24. This viscosity enhancement

is larger than with shorter chain for CF4-tails and/or the monovalent counterion Na^+ (**Figures 2 and 3**). At a water loading of W_0=10 the Ni^{2+} counterion surfactant led to higher viscosity than for Co^{2+}. In addition, the surfactants with longer ω-hydroperfluorocarbon-tails gave a higher of stability for W/CO_2 mixtures, and at lower CO_2 pressures/densities (**Figure 1**). These results suggest that ω-hydroperfluorocarbon-tails of > C_4 and divalent counterions important molecular features for CO_2-thickening surfactants.

(2) For most surfactant systems studied here, the relative viscosity η_{rel} was seen to have a maximum at W_0 = ~10 (**Figure 3**).

(3) In these W/CO_2 mixtures the reverse micelle morphology for Ni(di-HCF6)$_2$ and Co(di-HCF6)$_2$ surfactants changed from short rods at W_0=5 → long rods (rod length = ~260 Å) at W_0=10 → short rods or prorates at W_0=15 → spheres or oblates at W_0=20 (**Table 1**).

(4) Following on from (3), the aggregation number N_{agg} M(di-HCF6)$_2$ increased with increasing W_0 from 5 to 10 commensurate with the formation of long rod-like micelles, but decreased at $W_0 \geq 15$ owing to the formation of two-phase Winsor II systems (**Figures S22 and S23**).

(5) Rod-like reverse micelles with aspect ratios > 2.5 appeared at W_0 = 5-20 corresponding to effective surfactant packing parameters (EPP) = 1.1-1.8 (**Figure 5**).

Long rod-like reverse micelles are much more difficult to obtain in W/CO_2 systems than in W/O systems, and are only found with a few specialized FC-surfactants at low temperatures below 45 ºC [3-13,16-29,34-39]. As mentioned above, this study demonstrated successful formation of rod-like reverse micelles at a high temperature of 75 ºC close to reservoir conditions, and presented molecular design criteria for generating these. The surfactants studied here represent the most successful cases of low F-content additives and hence may make further impacts in this field. As such, long rod-like reverse micelles could offer a new generation of universal solvents with unique properties. Hopefully, the findings described here will be beneficial in the advancement of rod-like reverse micelle systems for CO_2-EOR and nanomaterial synthesis as well as in numerous other applications.

CRediT authorship contribution statement

M. Sagisaka : Supervision, Writing - original draft, review & editing, Y. Sato : Investigation, S. Kiani : Investigation, S. Alexander : Investigation, T. Ardyani: Investigation, A. Mohamed: Investigation, R. M. Enick : Methodology, S. E. Rogers : Investigation, C. Hill : Investigation, Writing - review & editing, J. Eastoe : Writing - review & editing,

Declaration of Competing Interest

There are no conflicts of interest to declare.

Acknowledgements

This project was supported by JSPS [KAKENHI, Grant-in-Aid for Scientific Research (B), No. 23H01750 and 19H02504, and International Exchanges 2021 Cost Share (JSPS) award 1845272]. We also acknowledge STFC for the allocation of beam time, travel, and consumables grants at ISIS. The authors acknowledge Shared Facility Center for Science and Technology, Hirosaki University (SFCST) for ^{1}H-NMR and FT-IR spectra measurements and elemental analysis. CH acknowledges JSPS for support as a JSPS International Research Fellow (Graduate School of Science and Technology, Hirosaki University).

Appendix A. Supplementary data

Supplementary data associated with this article can be found, in the online version at.

References

[1] E.J. Beckman, Supercritical and near-critical CO_2 in green chemical synthesis and processing, J. Supercrit. Fluids 28 (2004) 121-191.

[2] O. Massarweh, A. S. Abushaikha, A review of recent developments in CO_2 mobility control in enhanced oil recovery, Petroleum, 8 (2022) 291-317.

[3] S. Cummings, R. Enick, S. Rogers, R. Heenan, J. Eastoe, Amphiphiles for supercritical CO_2, Biochimie 94 (2012) 94-100.

[4] K.A. Consani, R.D. Smith, Observations on the solubility of surfactants and related molecules in carbon dioxide at 50 ºC, J. Supercrit. Fluids 3 (1990) 51-65.

[5] E.L.V. Goetheer, M.A.G. Vortaman, J.T.F. Keurentjes, Opportunities for process intensification using reverse micelles in liquid and supercritical carbon dioxide, Chem. Eng. Sci. 54 (**1999**) 1589-1596.

[5] W. Ryoo, S.E. Webber, K.P. Johnston, Water-in-carbon dioxide microemulsions with methylated branched hydrocarbon surfactants, Ind. Eng. Chem. Res. 42 (2003) 6348-6358.

[6] H. Lee, J.W. Pack, W. Wang, K.J. Thurecht, S.M. Howdle, Synthesis and phase behavior of CO_2-soluble hydrocarbon copolymer: poly(Vinyl Acetate-*alt*-Dibutyl Maleate), Macromolecules 43 (2010) 2276-2282.

[7] M. Sagisaka, K. Kudo, S. Nagoya, A. Yoshizawa, Highly methyl-branched hydrocarbon surfactant as a CO_2-philic solubilizer for water/supercritical CO_2 microemulsion, J. Oleo Sci. 62 (2013) 481-488.

[8] J. Eastoe, A. Mohamed, K. Trickett, S.Y. Chin, S. Cummings, M. Sagisaka, L. Hudson, S. Nave, R. Dyer, S. Rogers, R. Heenan, A universal surfactant for water, oils and CO_2, Langmuir 26 (2010) 13861–13866.

644 [9] M. Zulauf, H.F. Eicke, Inverted micelles and microemulsions in the ternary system water/aerosol-
645 OT/isooctane as studied by photon correlation spectroscopy, J. Phys. Chem. 83 (1979) 480–486.

646 [10] C.T. Jr. Lee, P.A. Psathas, K.P. Johnston, J. deGrazia, T.W. Randolph, Water-in-carbon dioxide
647 emulsions: formation and stability, Langmuir 15 (1999) 6781-6791.

648 [11] K.P. Johnston, K.L. Harrison, M.J. Klarke, S.M. Howdle, M.P. Heitz, F.V. Bright, C. Carlier, T.W.
649 Randolph, Water-in-carbon dioxide microemulsions: a new environment for hydrophiles including
650 proteins, Science 271 (1996) 624-626.

651 [12] R.G. Zielinski, S.R. Kline, E.W. Kaler, N.A. Rosov, Small-angle neutron scattering study of water
652 in carbon dioxide microemulsions, Langmuir 13 (1997) 3934-3937.

653 [13] E.D. Niemeyer, F.V. Bright, The pH within PFPE reverse micelles formed in supercritical CO_2, J.
654 Phys. Chem. B 102 (1998) 1474-1478.

655 [14] V.H. Dalvi, V. Srinivasan, P.J. Rossky, Understanding the effectiveness of fluorocarbon ligands in
656 dispersing nanoparticles in supercritical carbon dioxide, J. Phys. Chem. C 114 (2010) 15553-15561.

657 [15] V.H. Dalvi, V. Srinivasan, P.J. Rossky, Understanding the relative effectiveness of alkanethiol
658 ligands in dispersing nanoparticles in supercritical carbon dioxide and ethane, J. Phys. Chem. C 114
659 (2010) 15562-15573.

660 [16] M. Sagisaka, S. Iwama, A. Yoshizawa, A. Mohamed, S. Cummings, J. Eastoe, Effective and Efficient
661 Surfactant for CO_2 Having Only Short Fluorocarbon Chains, Langmuir 28 (2012) 10988-10996.

662 [17] M. Sagisaka, S. Yoda, Y. Takebayashi, K. Otake, B. Kitiyanan, Y. Kondo, N. Yoshino, K.
663 Takebayashi, H. Sakai, M. Abe, Preparation of a W/scCO_2 microemulsion using fluorinated surfactants,
664 Langmuir, 19 (2003) 220-225.

[18] M. Sagisaka, S. Yoda, Y. Takebayashi, K. Otake, Y. Kondo, N. Yoshino, H. Sakai, M. Abe, Effects of CO_2-philic tail structure on phase behavior of fluorinated Aerosol-OT analogue surfactant/water/supercritical CO_2 systems, Langmuir, 19 (2003) 8161-8167.

[19] M. Sagisaka, D. Koike, S. Yoda, Y. Takebayashi, T. Furuya, A. Yoshizawa, H. Sakai, M. Abe, K. Otake, Optimum tail length of fluorinated double-tail anionic surfactant for water/supercritical CO_2 microemulsion formation, Langmuir 23 (2007) 8784-8788.

[20] M. Sagisaka, S. Iwama, S. Ono, A. Yoshizawa, A. Mohamed, S. Cummings, C. Yan, C. James, S.E. Rogers, R.K. Heenan, J. Eastoe, Nanostructures in water-in-CO_2 microemulsions stabilized by double-chain fluorocarbon solubilizers", Langmuir, 29 (2013) 7618−7628.

[21] A. Mohamed, M. Sagisaka, F. Guittard, S. Cummings, A. Paul, S.E. Rogers, R.K. Heenan, R. Dyer, J. Eastoe, Low fluorine content CO_2-philic surfactants. Langmuir 27 (2011) 10562-10569.

[22] A. Mohamed, T. Ardyani, M. Sagisaka, S. Ono, T. Narumi, M. Kubota, P. Brown, C. James, J. Eastoe, A. Kamari, N. Hashim, I.M. Isa, S.A. Bakar, Economical and efficient hybrid surfactant with low fluorine content for the stabilization of water-in-CO_2 microemulsions, J. Supercrit. Fluids, 98 (2015) 127-136.

[23] D.C. Steytler, E. Rumsey, M. Thorpe, J. Eastoe, A. Paul, R.K. Heenan, Phosphate Surfactants for water-in-CO_2 microemulsions, Langmuir 17 (2001) 7948-7950.

[24] B. Xu, G.W. Lynn, J. Guo, Y.B. Melnichenko, G.D. Wignall, J.B. McClain, J.M. DeSimone, C.S. Johnston, Jr. NMR and SANS studies of aggregation and microemulsion formation by phosphorus fluorosurfactants in liquid and supercritical carbon dioxide, J. Phys. Chem. B 109 (2005) 10261-10269.

[25] K. Harrison, J. Goveas, K.P. Johnston, E.A. O'Rear III, Water-in-carbon dioxide microemulsions with a fluorocarbon-hydrocarbon hybrid surfactant, Langmuir 10 (1994) 3536-3541.

[26] A. Dupont, J. Eastoe, L. Martin, D.C. Steytler, R.K. Heenan, F. Guittard, E.T. Givenchy, Hybrid fluorocarbon-hydrocarbon CO_2-philic surfactants. 2. Formation and properties of water-in-CO_2 microemulsions, 20 (2004) 9960-9967.

[27] S. Cummings, D. Xing, R. Enick, S. Rogers, R. Heenan, I. Grillo, J. Eastoe, Design principles for supercritical CO_2 viscosifiers. Soft Matter 8 (2012) 7044–7055.

[28] M. Sagisaka, S. Ono, C. James, A. Yoshizawa, A. Mohamed, F. Guittard, S.E. Rogers, R.K. Heenan, C. Yan, J. Eastoe, Effect of fluorocarbon and hydrocarbon chain lengths in hybrid surfactants for supercritical CO_2, Langmuir 31 (2015) 7479-7487.

[29] M. Sagisaka, S. Ono, C. James, A. Yoshizawa, A. Mohamed, F. Guittard, R. M. Enick, S. E. Rogers, A. Czajka, C. Hill, J. Eastoe, Anisotropic reversed micelles with fluorocarbon-hydrocarbon hybrid surfactants in supercritical CO_2, Colloids and Surfaces B, 168 (2018) 201-210.

[30] D.H. Berry, W.B. Russel, The rheology of dilute suspensions of slender rods in weak flows, J. Fluid Mech. 180 (1987), 475-494.

[31] A.M. Wierenga, A.P. Philipse, Low-shear viscosity of isotropic dispersions of (Brownian) rods and fibres; a review of theory and experiments, Colloids Surf., A 137 (1998) 355−372.

[32] J. Gao, Z. Liu, M. J. Bentel, Y. Yu, Y. Men, J. Liu, Defluorination of Omega-Hydroperfluorocarboxylates (ω-HPFCAs): Distinct Reactivities from Perfluoro and Fluorotelomeric Carboxylates, Environmental Science & Technology 55 (2021) 14146-14155.

[33] X. Li, J. Turánek, P. Knötigová, H. Kudláčková, J. Mašek, S. Parkin, S.E. Rankin, B.L. Knutson, H.-J. Lehmler, Hydrophobic tail length, degree of fluorination and headgroup stereochemistry are determinants of the biocompatibility of (fluorinated) carbohydrate surfactants, *Colloid Surf. B* 73 (2009) 65-74.

[34] J. Eastoe, B.M.H. Cazelles, D.C. Steytler, J.D. Holmes, A.R. Pitt, T.J. Wear, R.K. Heenan, Water-in-CO_2 microemulsions studied by small-angle neutron scattering, Langmuir 13 (1997) 6980-6984.

[35] X. Dong, C. Erkey, H.-J. Dai, H.-C. Li, H.K. Cochran, J.S. Lin, Phase behavior and micelle size of an aqueous microdispersion in supercritical CO_2 with a novel surfactant, Ind. Eng. Chem. Res. 41 (2002) 1038-1042.

[36] J. Eastoe, A. Downer, A. Paul, D.C. Steytler, E. Rumsey, J. Penfold, R.K. Heenan, Fluoro-surfactants at air/water and water/CO_2 interfaces, Phys. Chem. Chem. Phys. 2 (2000) 5235-5242.

[37] J. Eastoe, A. Paul, A. Downer, D.C. Steytler, E. Rumsey, Effects of fluorocarbon surfactant chain structure on stability of water-in-carbon dioxide microemulsions. Links between aqueous surface tension and microemulsion, Langmuir 18 (2002) 3014-3017.

[38] K. Trickett, D. Xing, R. Enick, J. Eastoe, M.J. Hollamby, K.J. Mutch, S.E. Rogers, R.K. Heenan, D.C. Steytler, Rod-like micelles thicken CO_2, Langmuir 26 (2010) 83-88.

[39] S. Cummings, K. Trickett, R. Enick, J. Eastoe, CO_2: a wild solvent, tamed, Phys. Chem. Chem. Phys. 13 (2011) 1245-1696.

[40] M. P. Hochstein, Assessment and modelling of geothermal reservoirs (small utilization schemes), Geothermics 17 (1988) 15-49.

[41] R. Span, W. Wagner, A New Equation of State for Carbon Dioxide Covering the Fluid Region from the Triple-Point Temperature to 1100 K at Pressures up to 800 MPa. J. Phys. Chem. Ref. Data 25 (1996) 1509-1596.

[42] J. Pfitzner, Poiseuille and his law, Anaesthesia, 3 (1976) 273-275

[43] A. Fenghour, W. A. Wakeham, V. Vesovic, The Viscosity of Carbon Dioxide, J. Phys. Chem. Ref. Data 27 (1998) 31–44.

[44] E. S. Menon, Chapter Five - Fluid Flow in Pipes, Transmission Pipeline Calculations and Simulations Manual, (2015) 149-234.

[45] R. Darby, Chemical Engineering Fluid Mechanics (2nd ed.). CRC Press. Ron (2001) 64.

[46] Merck Index. 11th Edition. Merck & Company, Inc., Rahway, NJ; 1989.

[47] M. Kotlarchyk, S.-H. Chen, J.S. Huang, M.W. Kim, Structure of three-component. Microemulsions in the critical region determined by small angle neutron scattering data, Phys. Rev. A 29 (1984) 2054-2069.

[48] J. C. Eriksson, S. Ljunggren, Thermodynamic Evaluation of the Polydispersity of Droplet Microemulsions, Langmuir 11 (1995) 1145–1153.

[49] M. Sagisaka, S. Iwama, S. Hasegawa, A. Yoshizawa, A. Mohamed, S. Cummings, S. E. Rogers, R. K. Heenan, J. Eastoe, Super-efficient surfactant for stabilizing water-in-carbon dioxide microemulsions, Langmuir 27 (2011) 5772–5780.

[50] A. Guinuier, G. Fournet, Small-Angle Scattering of X-Rays, Wiley, New York, 1956.

[51] M. Porras-Gomez, C. Leal, Lipid-based Liquid Crystalline Films and Solutions for the Delivery of Cargo to Cells, Liq. Cryst. Rev. 7 (2019) 167-182.

[52] J.N. Israelachvili, Measurements of hydration forces between macroscopic surfaces, Chem. Scr. 25 (1985) 7-14.

[53] C. Hill, Y. Umetsu, K. Fujita, T. Endo, K. Sato, A. Yoshizawa, S. E. Rogers, J. Eastoe, M. Sagisaka, Design of Surfactant Tails for Effective Surface Tension Reduction and Micellization in Water and/or Supercritical CO_2, Langmuir, 36 (2020) 14829–14840.

[54] S. Nave, J. Eastoe, R.K. Heenan, D. Steytler, I. Grillo, What is so special about Aerosol-OT? 2. Microemulsion systems, Langmuir 16 (2000) 8741-8748.

[55] A. El Aferni, M. Guettari, T. Tajouri, Determination of the Water/AOT/Isooctane Reverse Micelles Size Parameters from Their Refractive Index Data, Journal of Solution Chemistry, 46 (2017) 89–102.

[56] K. D. Danov, P. A. Kralchevsky, S. D. Stoyanov, J. L. Cook, I. P. Stott, E. G. Pelan, Growth of wormlike micelles in nonionic surfactant solutions: Quantitative theory vs. experiment, Advances in Colloid and Interface Science, 256 (2018) 1-22.

[57] M. Pleines, W. Kunz, T. Zemb, Understanding and Prediction of the Clouding Phenomenon by Spontaneous and Effective Packing Concepts. J. Surfactants Deterg, 22 (2019) 1011-1021,

[58] J. F. Ontiveros, C. Pierlot, M. Catté, V. Molinier, A. Pizzino, J. L. Salager, J. M. Aubry, Classification of Ester Oils According to Their Equivalent Alkane Carbon Number (EACN) and Asymmetry of Fish Diagrams of $C_{10}E_4$/Ester Oil/Water Systems. J. Colloid Interface Sci. 403 (2013) 67–76.

[59] R. Nagarajan, Molecular Packing Parameter and Surfactant Self-Assembly: The Neglected Role of the Surfactant Tail. Langmuir, 18 (2002) 31–38.